Giant magnetoresistance effect in a magnetic-electric barrier structure

Feng Zhai,[1,2,*] Yong Guo,[1] and Bing-Lin Gu[1]
[1] *Department of Physics, Tsinghua University, Beijing 100084, China*
[2] *Center for Advanced Study, Tsinghua University, Beijing 100084, China*
(Received 28 May 2002; published 4 September 2002)

A spin-independent giant magnetoresistance effect is demonstrated in a magnetically modulated two-dimensional (2D) electron gas, which can be realized by depositing two parallel ferromagnets on top of the heterostructure. The transmission for the parallel and antiparallel magnetization configurations shows a quite distinct dependence on the longitudinal wave vector of the incident electrons. Such a discrepancy results in a tremendous magnetoresistance (MR) ratio, which can be up to 10^6% for a realistic electron density. It is confirmed that the MR ratio can be further tuned by the inclusion of an electric barrier. In addition, studies indicate that the structure with antiparallel magnetization arrangement can be used to collimate the 2D electron beam.

DOI: 10.1103/PhysRevB.66.125305 PACS number(s): 73.40.−c, 75.75.+a, 72.20.−i, 73.23.−b

The discovery of the so-called giant magnetoresistance (GMR) effect[1] has given rise to a tremendous economic impact on magnetic information storage.[2] Fueled by its fascinating practical applications such as ultrasensitive magnetic field sensors, read heads, and random access memories, numerous theoretical and experimental studies have devoted to dealing with the GMR phenomenon.[3] The structures where GMR is observed generally consist of ferromagnetic layers separated by thin nonmagnetic layers. In such heterogeneous systems, GMR is characterized by a striking drop of the electric resistance when an external magnetic field switches the magnetizations of adjacent magnetic layers from an antiparallel (AP) alignment to a parallel (P) one. It is widely agreed that the spin-dependent scattering of electronic carriers results in different values (G_P and G_{AP}) of the conductances in the two configurations.[4] The magnetoresistance (MR) ratio is usually defined as the corresponding normalized difference, i.e., $\mathrm{MR}=(G_P-G_{AP})/G_{AP}$.

To manufacture high-quality magnetic sensors and read heads, one requires systems with high MR ratio under relatively low switching magnetic fields. In conventional GMR devices, the nonmagnetic spacer is a single metal and the current flows in the plane (CIP). The sample in such a geometry has macroscopic size and thus obvious resistance. At low temperatures, high values of the MR ratio up to 220% have been reported, but with sizable magnetic fields.[5] The CPP (current perpendicular to the plane) geometry is theoretically more effective at filtering the current, which usually leads to a larger GMR than the CIP counterpart. However, the exceedingly small resistance involved in the CPP configuration makes the measurements more dedicated. According to the recent report,[6] this difficulty may be overcome by using perioducally modulated spacers.

It seems that the spin-dependent transport is indispensable for the observation of the GMR. Here we propose an alternative way to realize the GMR effect, which, however, makes no use of the spin freedom of the electrons. The considered system is a two-dimensional electron gas (2DEG) in the (x,y) plane modulated by a perpendicular magnetic field B_z and an electric barrier U. The magnetic field is created by the deposition, on top of the heterostructure, of two parallel metallic ferromagnetic stripes with widths d and magnetizations along the x axis. A suitable external magnetic field can change the relative orientation of the two magnetizations, which is antiparallel at zero field. The fringe field of each ferromagnet induces a positive B_z underneath one edge of the stripe and a negative B_z underneath the other edge.[7] At the limit of a small distance between the 2DEG and the ferromagnets, the magnetic barrier can be approximated by delta functions, i.e., $B_z(x)=Bl_{B_0}\{[\delta(x)-\delta(x-d)]+\gamma[\delta(x-d-D)-\delta(x-L)]\}$. Here, B gives the strength of the magnetic field, $l_{B_0}=\sqrt{\hbar/eB_0}$ is the magnetic length for an estimated magnetic field B_0, γ represents the magnetization configuration (± 1 or P, AP), D is the distance between two stripes, and $L=2d+D$ is the total length of the structure along the current direction (x). The model magnetic field configurations for $\gamma=\pm 1$ are schematically depicted in Fig. 1. Further, when a negative voltage is applied to the stripes, an electric barrier arises. For simplicity, the latter is taken as a square shape[8] with height U_0, i.e., $U(x)=U_0\Theta(x)\Theta(L-x)$, where $\Theta(x)$ is the Heaviside step function.

In the framework of the effective-mass approximation, the Hamiltonian of such a system can be written as

$$H=\frac{1}{2m^*}[\mathbf{P}+e\mathbf{A}(\mathbf{x})]^2+U(x)+g^*\mu_B B_z(x)\sigma_z/2, \quad (1)$$

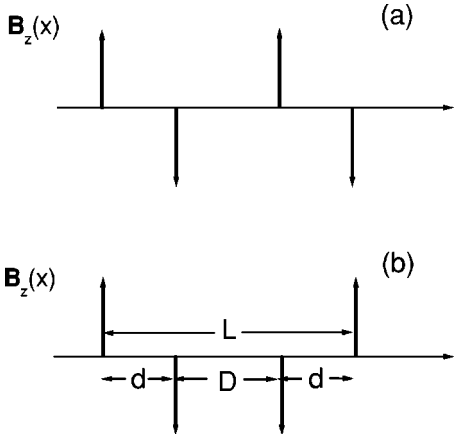

FIG. 1. The model magnetic field profile for the parallel (a) and antiparallel (b) configurations of two magnetic moments.

where m^* is the effective mass of the electron, e is the absolute value of the electron's charge, $\mathbf{P}$ is the momentum operator, $\mathbf{A}(x)=(0, A(x), 0)$ is the vector potential in the Landau gauge, g^* is the effective g factor of the electron, μ_B the Bohr magneton, and $\sigma_z=+1/-1$ for electrons with up/down spin. Using the cyclotron frequency $\omega_c=eB_0/m^*$ and the magnetic length l_{B_0}, we express all quantities in dimensionless units, for example, (1) the magnetic field $\mathbf{B}_z(x) \rightarrow B_0\mathbf{B}_z(x)$, (2) the vector potential $\mathbf{A}(x)\rightarrow B_0 l_{B_0}\mathbf{A}(\mathbf{x})$, (3) the energy $E\rightarrow\hbar\omega_c E$, and (4) the coordinate $\mathbf{r}\rightarrow l_{B_0}\mathbf{r}$ and (the wave vector) $\mathbf{k}\rightarrow l_{B_0}^{-1}\mathbf{k}$. For the GaAs 2DEG and a realistic value $B_0=0.2$ T, we have $m^*=0.067\ m_0$ (m_0 is the free electron mass), $g^*=0.44$, $l_{B_0}=575$ Å, and $E_0=\hbar\omega_c=0.34$ meV. The total wave function describing an electron with incident energy E can be written as a product $\Phi(x,y)=e^{ik_y y}\Psi(x)$, where $\Psi(x)$ satisfies the reduced one-dimensional Schrödinger equation

$$-\frac{1}{2}\frac{d^2\Psi}{dx^2}+U_{eff}(x,k_y)\Psi=E\Psi. \tag{2}$$

It is going to be useful to introduce the effective potential of the magnetic-electric barrier:

$$U_{eff}(x,k_y)=\frac{1}{2}[k_y+A(x)]^2+U(x) + (g^*m^*/2m_0)B_z(x)\sigma_z/2. \tag{3}$$

The last term in Eq. (3) represents the Zeeman coupling between the electronic spin and the local magnetic field.[9] Comparing to other terms in U_{eff}, the absolute value of such a term is much smaller (the ratio between them is estimated as $g^*m^*/2m_0=0.015\ll 1$). Therefore, the spin-dependent term plays a minor role in determining the transport properties of electrons and can be omitted. Our numerical results also confirm this point. In contrast, the effective potential depends strongly not only on the longitudinal wave vector k_y, but also on the profile of the local magnetic field. The k_y dependence renders the motion an essentially two-dimensional process.[10,11] From the expression of the vector potential $A(x)=B[\Theta(x)\Theta(d-x)+\gamma\Theta(x-d-D)\Theta(L-x)]$, one can see that when the P alignment ($\gamma=1$) turns to the inverse ($\gamma=-1$), U_{eff} varies substantially. It is the dependence on the magnetic profile of U_{eff} that leads to the GMR in the involving system. Further, the GMR effect is tunable if the electric barrier is included.

We adopt the scattering-matrix method[12] to evaluate the transmission coefficient $T_\gamma(E,k_y)$ ($\gamma=P/AP$). The ballistic conductance is calculated by averaging the electron flow over half the Fermi surface[13]:

$$G_\gamma(E_F)=G_0\int_{-\pi/2}^{\pi/2}T_\gamma(E_F,\sqrt{2E_F}\sin\theta)\cos\theta d\theta, \tag{4}$$

with θ the incident angle relative to the x direction. The conductance is presented in units of $G_0=2e^2m^*v_F L_y/h^2$, where L_y is the longitudinal length of the structure and v_F the Fermi velocity.

Fig. 2 presents the transmission through a magnetic-electric barrier with P alignment. The longitudinal wave vectors are set to be $k_y=0$ in the left panel and $k_y=\pm 2$ in the right one. In all of the graphs, we use the magnetic structure parameters $B=5$, $d=1$, and $D=3$. Note that the transmission spectrum demonstrates obvious anisotropy with k_y.[10,11] For suitable negative k_y values (such as $k_y=-2$), the reflection is almost complete for low incident energy. Beyond this forbidden region, the transmission shows obvious oscillations and approaches unity rapidly. For $k_y\geqslant 0$, however, there exist several line-shaped resonant peaks with unity values before the oscillation occurs. In addition, the presence of an electric barrier significantly alters the positions of the transmission peaks and minima.

All of the features stated above reflect the structure of the potential U_{eff} to some extent. For a pure magnetic barrier ($U_0=0$) with the P alignment and in the case $k_y>-B/2$, U_{eff} has a symmetric double-barrier structure and the middle region between two ferromagnets acts as a quantum well. When the barriers are high enough, the process of electron motion is tunneling through the double barriers. The transmission is thus generally blocked while the sharp peaks correspond to the resonant tunneling, which occurs when the incident energy coincides with one of quasibound energy levels within the well. For barriers lower than the first intrawell virtual state, however, no resonance appears when the energy falls below the barriers. In the case of $k_y<-B/2$, U_{eff} consists of symmetric double wells, which are usually transparent for electrons. Further, the electric barrier lifts all quasibound levels and makes the structure more opaque to electrons.

In the following, we examine the transmission characteristics for the AP alignment, which are exhibited in Fig. 3. In the case of normal incidence ($k_y=0$), the transmission curve for the AP alignment is exactly the same as that for the P alignment because their corresponding effective potentials are identical. In addition, the effective potential of the AP configuration has an even symmetry about the center, i.e., $U_{eff}(x-L/2,k_y)=U_{eff}(L/2-x,-k_y)$. As we know, for particles traversing a potential in opposite directions the transmission is always equal. Therefore, such a symmetry results in the invariance of the transmission with respect to the replacement $k_y\rightarrow -k_y$. It is thus sufficient in Fig. 3 to take only positive k_y values into account. For a pure magnetic barrier with the AP alignment, electrons with $k_y<B/2$ feel an asymmetric electric double-barrier potential. For small k_y values the height difference of two barriers is slight, so one can observe some sharp incomplete resonances in the low-energy region (see the solid line for $k_y=0.7$). With k_y increasing, these peaks vanish and the transmission is blocked when the incident energy is below the higher barrier. In the case of $k_y>B/2$, U_{eff} consists of a barrier and a well. The tunneling properties are mainly determined by the barrier. As a result, the transmission for large k_y (for example, $k_y=4$) may be strongly suppressed in the whole considered energy region. From these facts one can conclude that for a given incident energy, only electrons with small $|k_y|$ values have finite transmission through the same structure with AP arrangement. Therefore, such a device can be used to collimate the 2D electron beam. The (positive) electric barrier in-

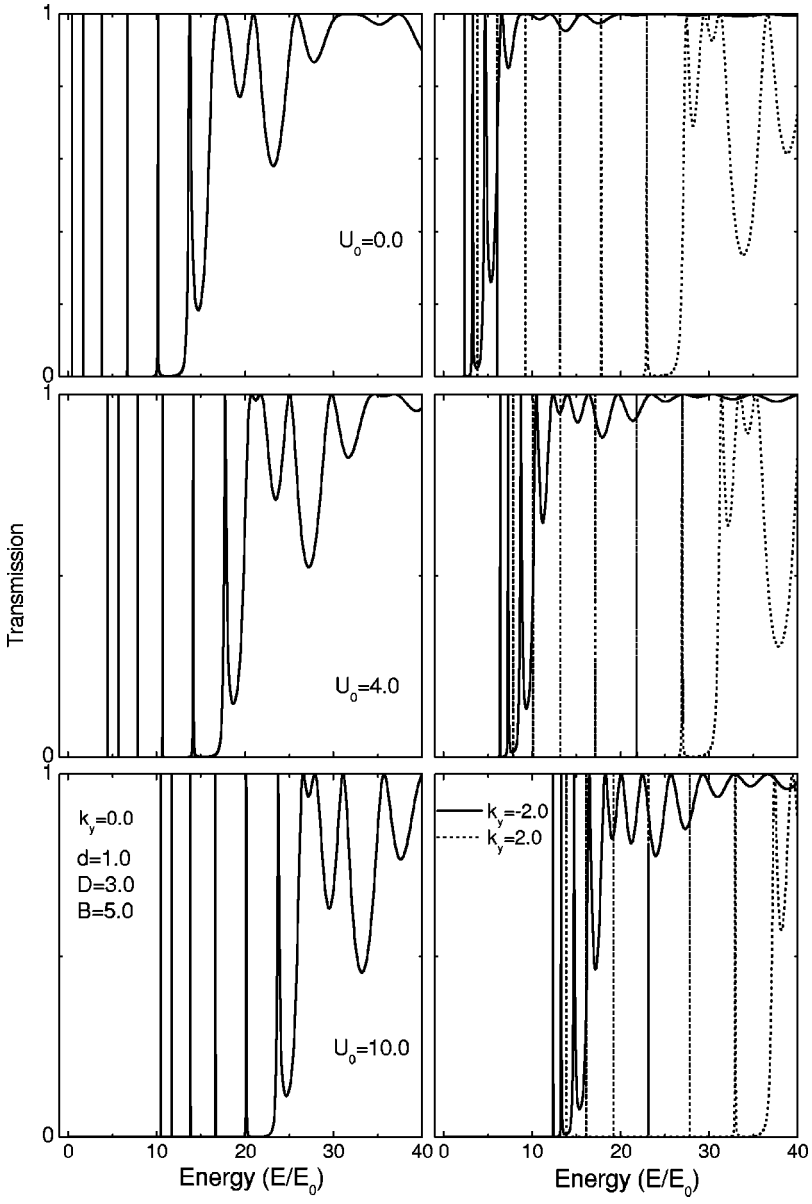

FIG. 2. Transmission through a magnetic-electric barrier with parallel magnetizations for $k_y=0$ (left panel) and $k_y=\pm 2$ (right panel). The magnetic structure parameters are $B=5.0$, $d=1$, and $D=3$. The height of the electric barrier is taken as $U_0=0$, 4, and 10.

creases the height of the effective barrier(s) and extends the forbidden region of the transmission, as depicted in the inset of Fig. 3.

As demonstrated above, the transmission for two alignments (P/AP) is quite distinct. Now we see to what extent such a difference is reflected in the measurable quantity, the conductance G. Fig. 4 shows the conductance versus the Fermi energy for different heights of the electric barrier. Within the low-energy region, for both P and AP alignments the magnetic barrier blocks the transmission drastically and the corresponding conductance is almost zero. The blocking effect is more obvious for the AP alignment. So there exists a wide energy region where G_{AP} is closed to zero whereas G_P is finite. Beyond the transmission-blocked region, G_P exhibits rapid increase essentially with the Fermi energy increasing. In addition, in the G_P-E_F curve one can see a striking conductance peak with a large peak-to-valley ratio as well as several small peaks. For the AP alignment, there also exists a sharp conductance peak. However, in the vicinity of this peak, the conductance decays rapidly to zero. Note that in the G_{AP}-E_F curve several weak peaks appear within the transmission-blocked region. A positive electric barrier drives all peaks moving towards the high-energy region and lowers the whole conductance curve. All of these features originate from the rich resonant transmission behaviors of the considered magnetic-electric barrier.

To see the discrepancy between G_P and G_{AP} more clearly, in Fig. 5 we present the magnetoresistance ratio as a function of the Fermi energy. The concerned energy region is exactly the same as that in Fig. 4. It is remarkable that the MR ratio shows drastic oscillations with the Fermi energy. When E_F exceeds $10E_0$, the MR ratio for a pure magnetic barrier is lower than $10^5\%$ and decays rapidly to the magnitude of $10^2\%$. For a typically electron density $n_e \approx 10^{11}$ cm^{-2} in GaAs 2DEG which gives $E_F=3.55$ meV$\approx 10E_0$, the corresponding MR ratio is relatively small. However, if an electric barrier with height $U=4E_0\approx 1.4$ meV is included, it can be up to $5\times 10^6\%$. The high values of the MR ratio are mainly

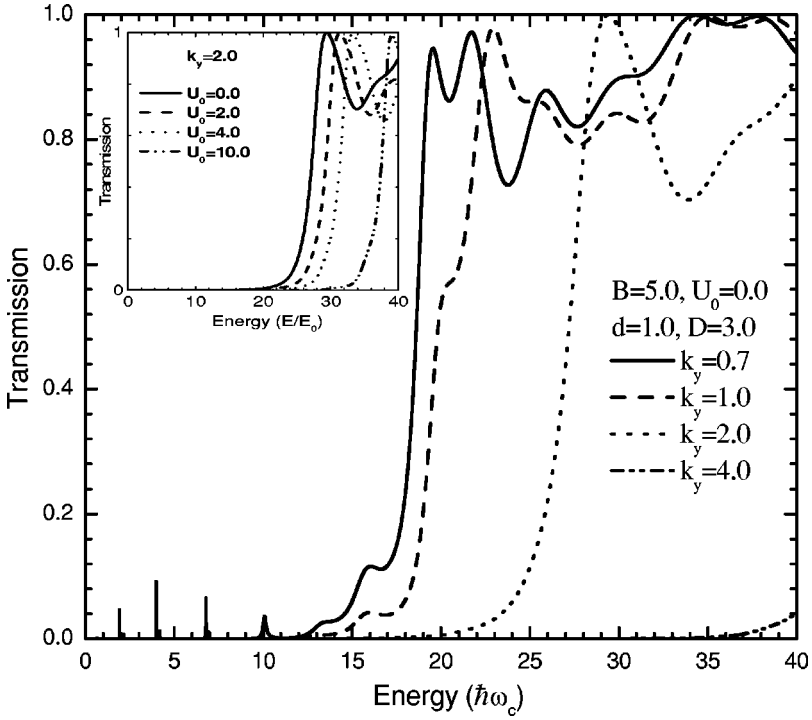

FIG. 3. Transmission through a pure magnetic barrier with antiparallel magnetizations for different values of electron momentum $k_y=0.7$, 1, 2, and 4. The magnetic structure parameters are the same as those in Fig. 2. The inset presents the energy dependence of the transmission for different values of the electric barrier height with $k_y=2$.

due to the strong suppression of the transmission in the AP alignment. The electric barrier changes the degree of the suppression and thus can be used to adjust the MR ratio. The latter is obviously reflected in the inset of Fig. 5. From this inset one can see that for a fixed E_F ($=15E_0$), the MR ratio is small for negative U_0 and shows obvious oscillations and deep valleys for positive U_0. The valleys correspond to the weak conductance peaks in the G_{AP}-E_F curves.

All the results presented so far are obtained in the case of zero temperature. However, one can expect that such a kind of GMR device also operates at room temperature if a proper electric barrier is chosen. As we know, at a finite temperature T the main contribution to the ballistic conductance comes from electrons with energy located in the region (E_F-k_BT, E_F+k_BT). If the electric barrier is taken as a double-barrier form $U(x)=U_0[\Theta(x)\Theta(d-x)+\Theta(x-d-D)\Theta(L-x)]$ and $U_0>E_F+k_BT$, resonant tunneling is the dominant transport mechanism and the distinction of the transmission between the P and AP alignments still exists. So the GMR effect may survive (though much smaller than the case of

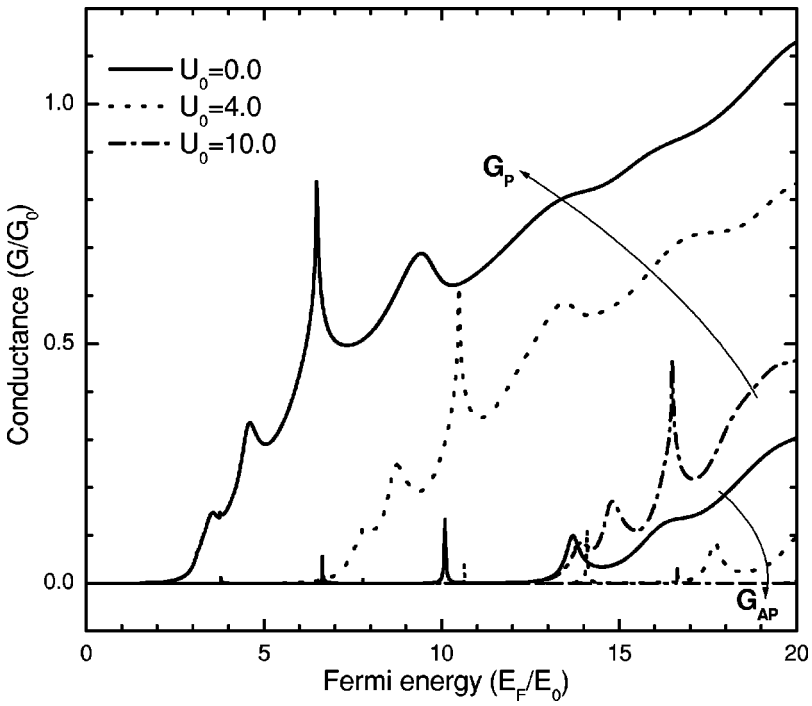

FIG. 4. The conductance of electrons as a function of the Fermi energy for both P and AP alignments under different electric barrier heights $U_0=0$, 4, and 10. The magnetic structure parameters are the same as those in Fig. 2.

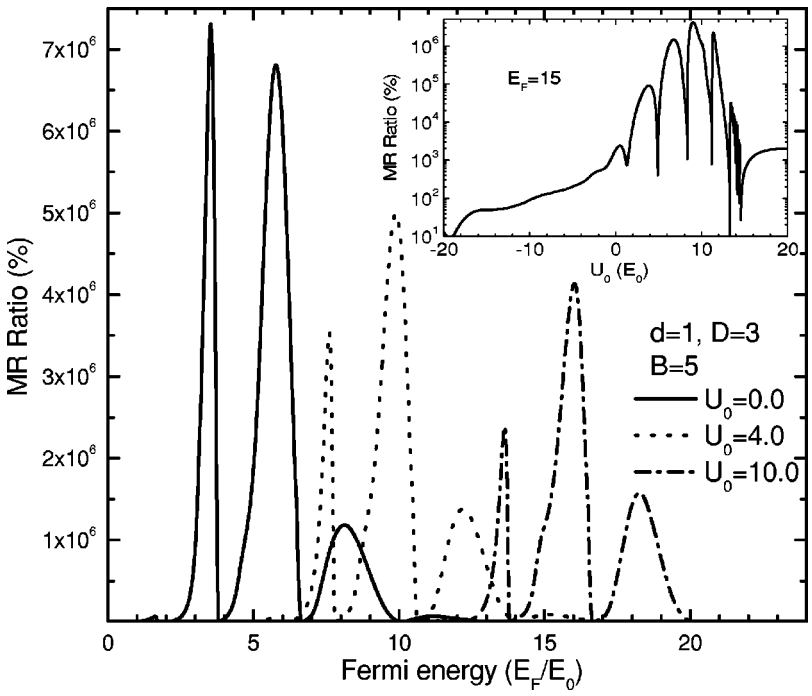

FIG. 5. The MR ratio vs the Fermi energy. The magnetic structure parameters are the same as those in Fig. 2. In the inset the MR ratio is shown as a function of the electric barrier height for a fixed Fermi energy $E_F = 15$.

$T = 0$) at finite temperature for the typical Fermi energy. For practical utility, it is necessary to take a step further to investigate other effects on the MR ratio, which include the temperature, realistic scattering rates, disorder, and so on. Such works are now in progress.

In summary, we have investigated the ballistic transport in a 2DEG subject to a combined magnetic-electric barrier, where the magnetic barrier is created by depositing two parallel ferromagnetic stripes with magnetizations along the current direction. The results indicate that the difference of wave-vector-dependent transmission for two magnetization configurations (P/AP) leads to a tremendous MR ratio, which can approach 10^6% for a realistic electron density and can be further adjusted by an electric barrier. Unlike metal-based GMR devices where the GMR is caused by spin-dependent scattering, here the ferromagnets just generate a modulated local field and electronic spin plays a minor role in the ballistic transport because of a small g factor in the GaAs 2DEG. Due to its obviously measurable electric resistance and low switching magnetic field (~ 1 T), such a semiconductor-based GMR structure is an ideal candidate for magnetic reading devices. Of course, it is also in the realizable scope of current technological advances. In addition, the structure with AP alignment is shown to suppress the transmission for electrons with large incident angle and thus can be used to collimate the 2D electron beam.

This work was supported by the National Natural Science Foundation of China (Grant No. 10004006) and by the National Key Project of Basic Research Development Plan (Grant No. G2000067107).

*Electronic address: fzhai@castu.tsinghua.edu.cn

[1] M.N. Baibich, J.M. Broto, A. Fert, F. Nguyen Van Dau, F. Petroff, P. Etienne, G. Creuzet, A. Friederich, and J. Chazelas, Phys. Rev. Lett. **61**, 2472 (1988).

[2] G.A. Prinz, Science **282**, 1660 (1998).

[3] For a review, see P.M. Levy, Solid State Phys. **47**, 367 (1994); M.A.M. Gijs and G.E.W. Bauer, Adv. Phys. **46**, 285 (1997); J-Ph. AnSermet, J. Phys.: Condens. Matter **10**, 6027 (1998).

[4] K.M. Schep, P.J. Kelly, and G.E.W. Bauer, Phys. Rev. B **57**, 8907 (1998).

[5] R. Schad, C.D. Potter, P. Belien, G. Verbanck, V.V. Moshchalkov, and Y. Bruynseraede, Appl. Phys. Lett. **64**, 3500 (1994).

[6] M.S. Ferreira, J. d'Albuquerque e Castro, R.B. Muniz, and M. Villeret, Appl. Phys. Lett. **75**, 2307 (1999).

[7] V. Kubrak, F. Rahman, B.L. Gallagher, P.C. Main, M. Henini, C.H. Marrows, and M.A. Howson, Appl. Phys. Lett. **74**, 2507 (1999); T. Vanč ura, T. Ihn, S. Broderick, K. Ensslin, W. Wegscheider, and M. Bichler, Phys. Rev. B **62**, 5074 (2000).

[8] G. Papp and F.M. Peeters, Appl. Phys. Lett. **78**, 2184 (2001); H.Z. Xu and Y. Okada, *ibid.* **79**, 3119 (2001); Y. Guo, F. Zhai, B.L. Gu, and Y. Kawazoe, Phys. Rev. B **66**, 045312 (2002).

[9] The correct form of the Zeeman term was presented by G. Papp and F.M. Peeters, Appl. Phys. Lett. **79**, 3198 (2001).

[10] A. Matulis, F.M. Peeters, and P. Vasilopoulos, Phys. Rev. Lett. **72**, 1518 (1994).

[11] Y. Guo, B.L. Gu, W.H. Duan, and Y. Zhang, Phys. Rev. B **55**, 9314 (1997); Y. Guo, B.L. Gu, Z.Q. Li, J.Z. Yu, and Y. Kawazoe, J. Appl. Phys. **83**, 4545 (1998); Y. Guo, H. Wang, B.L. Gu, and Y. Kawazoe, Phys. Rev. B **61**, 1728 (2000).

[12] See, for example, M. Cahay, M. McLennan, and S. Datta, Phys. Rev. B **37**, 10 125 (1988); H. Xu, *ibid.* **50**, 8469 (1994).

[13] M. Büttiker, Phys. Rev. Lett. **57**, 1761 (1986).